ACOUSTIC DATA ANALYSIS AND MODELS OF KRILL SPATIAL DISTRIBUTION

A. Morin, A. Okubo and K. Kawasaki

Abstract

Acoustic data obtained on 4-5 January 1987 aboard the R/V *Professor Siedlecki* were used in three descriptors of krill spatial aggregation: power spectra for krill biomass fluctuations in space, semivariogram (spatial autocorrelation of krill biomass) and the frequency distribution of krill biomass estimate. The wavenumber spectrum resembles a white noise at scales of 2-20 km, although at scales smaller than 1 km the spectrum appears to lose its power significantly. The semivariance of biomass does not vary significantly over most distances between points except for the distances smaller than 1 km. The computed frequency distribution of krill biomass is bimodal and appears to be the mixture of two lognormal distributions. These two distributions may correspond to the between and within patch biomass. These results of data analysis suggest that krill patch size or rather a basic swarm size should be smaller than 200 m, finest resolution of our data analyzed, and the real spatial distribution of krill should be the manifestation of the balance between the dispersion of the basic swarm units and long-range density-dependent attraction of the units. Simple dynamical and kinematical models can interpret the observed result.

Résumé

Les données acoustiques recueillies les 4 et 5 janvier 1987 à bord du navire de recherche *Professor Siedlecki* ont été utilisées dans trois descripteurs de répartition spatiale du krill: spectre d'intensité pour les fluctuations de la biomasse du krill dans l'espace, semivariogramme (autocorrélation spatiale de la biomasse du krill) et distribution de fréquences de la biomasse estimée de krill. Le spectre à ondes ressemble à un son blanc aux échelles de 2 à 20 km, mais aux échelles inférieures à 1 km, le spectre semble diminuer considérablement en intensité. La semivariance de la biomasse ne varie pas de manière significative pour la plupart des distances entre les points, sauf pour les distances inférieures à 1 km. La distribution calculée des fréquences de la biomasse du krill est bimodale et semble consister en un mélange de deux distributions logarithmiques normales. Ces deux distributions pourraient correspondre à la biomasse à l'intérieur d'un regroupement, d'une part, et entre les regroupements, d'autre part. Ces résultats de l'analyse des données suggèrent que la taille d'un regroupement de krill, ou plutôt la taille de base d'un banc, devrait être inférieure à 200 m, résolution la plus précise de nos données analysées, et que la répartition spatiale réelle du krill devrait être la manifestation de l'équilibre entre la dispersion des unités de base des bancs et l'attraction des unités à longue portée et dépendant de la densité. Des modèles dynamiques et cinématiques simples peuvent interpréter le résultat observé.

Резюме

Акустические данные, полученные R/V *Professor Siedlecki* 4-5 января 1987 г., использованы в трех типах описания пространственной агрегации криля: спектральной функции пространственных флуктуаций биомассы криля, графике полумногообразия (пространственной автокорреляции биомассы криля) и частотном распределении оценочных величин биомассы криля. В диапазоне 2-20 км спектр волновых чисел напоминает белый шум, хотя в диапазоне меньше 1 км в спектре наблюдается значительная потеря энергии. Полумногообразие массы существенно не меняется при почти любых расстояниях между точками, за исключением расстояний меньше 1 км. Вычисленное частотное распределение биомассы криля оказывается бимодальным и, видимо, является смесью двух типов логнормального распределения. Эти два типа распределения могут соответствовать биомассе между пятнами и биомассе внутри пятна. Полученные результаты анализа данных заставляют предположить, что размер пятна криля, или вернее размер типичного скопления криля должен быть меньше 200 м, - что является пределом разрешающей способности при получении подвергнутых нами анализу данных, и что реальное пространственное распределение криля должно отразить имеющийся баланс между дисперсией типичных скоплений и взаимным привлечением отдельных элементов скопления с большого расстояния, - в зависимости от плотности скопления. Полученные результаты можно интерпретировать с помощью простых динамических и кинематических моделей.

Resumen

Se utilizaron los datos acústicos, obtenidos el 4-5 de enero de 1987 a bordo del B/I *Professor Siedlecki*, en tres descriptores de concentración espacial del krill: densidad espectral de las fluctuaciones espaciales de la biomasa del krill, semivariograma (autocorrelación espacial de la biomasa del krill), y distribución de frecuencias en la estimación de la biomasa del krill. A escalas de 2-20 km, el espectro del número de ondas se parece a un ruido blanco, aunque a escalas menores de 1 km el espectro parece perder su potencia de modo significativo. El semivariograma de la biomasa no parece variar considerablemente en la mayoría de distancias entre puntos, excepto en las distancias menores de 1 km. La distribución de frecuencias calculada de la biomasa del krill es bimodal, y parece ser la combinación de dos distribuciones logarítmicas normales. Estas dos distribuciones pueden corresponder a la biomasa existente dentro de una mancha y entre varias. Estos resultados, obtenidos del análisis de datos, hacen pensar que el tamaño de las manchas de krill, o mejor dicho, el tamaño de un cardumen de krill debería ser menor de 200 m, la resolución más precisa del análisis de nuestros datos, y la distribución espacial real del krill debería ser la manifestación del

equilibrio entre la dispersión de las unidades de cardumen básicas y la atracción a largo alcance dependiente de la densidad de dichas unidades. Modelos dinámicos y kinemáticos sencillos pueden interpretar este resultado observado.

1. INTRODUCTION

The Antarctic krill (*Euphausia superba*) constituting nearly half of the Antarctic zooplankton biomass (Brinton and Antezana 1984), is the dominant herbivores and plays an important role in supporting animal populations such as whales, seals and penguins as well as fish. Krill distribution is highly variable in space and time (Marr 1962), and krill often aggregates into dense swarms, ranging from square meters to vast super swarms, but spherical or laminar swarms of volume 1-10 m^3 may be quite common (Mauchline 1980).

Recently Weber et al. (1986) have used the techniques of spectral analysis to examine the spatial scale dependence of variability in temperature, phytoplankton (chlorophyll-a) and krill biomass in the Antarctic Ocean south of Africa. They found that the power spectra for temperature and chlorophyll fluctuations differed markedly from that of krill biomass. In other words, the spectra of temperature and chlorophyll appeared very similar, and the mean slopes of the temperature and chlorophyll spectra, when plotted on a log-log plot, were -1.66 and -2.04, respectively, whereas the krill spectra were much flatter with near-zero slopes, indicating an approximately equal variance at all scales (white noise).

The result of Weber et al. (1986) implies that mechanisms controlling temperature and chlorophyll spatial distributions are different from those for krill distributions. The spectral slope of -1.66 is quite consistent with the -5/3 power predicted by Kolmogorov (1941) for the inertial subrange of turbulence, and also the slope of -2 for chlorophyll may be interpreted by the turbulence model with a slight modification by biological activities (Fasham, 1978). For krill, a purely physical model would be inappropriate in explaining their high variability at small scales. Although krill distribution is influenced by large scale physical processes, other biological factors, presumably behaviour, must be responsible for the high heterogeneity at small scales. Thus a krill distribution model would have to include additional mechanisms acting predominantly at small scales.

The first step of our approach is to examine the krill biomass distribution in the vicinity of King George Island through spectral analysis, and compare the resulting power spectrum with the description of Weber et al (1986) to see if the same type of spectrum can describe the krill distribution patterns in different areas. Acoustic data provided by M.C. Macaulay were used in our spectral analysis. The same data were also used to compute the semivariogram (Mackas 1984) for further investigation of the spatial variability in krill biomass. The third description is the frequency distribution of biomass estimate, another measure of patchiness in the krill distribution.

2. METHODS

Acoustic data (so-called "Macaulay data") obtained on 4-5 January 1987 aboard the R/V *Professor Siedlecki* were used in the following analysis (Figure 1). The data tapes contained continuous reading of estimated average krill biomass (g/m^3; 200 k kHz estimates) at each meter of depth ranging from 3 to 185 m at a horizontal resolution of approximately 200 m for 8 transects. Vertical profiles were summed to obtain an areal estimate of krill biomass (g/m^2). The resulting traces were then subdivided into 16 series of 64 data points for spectral analysis. The power at each frequency for the 16 transects was then summed and normalized to the total power of the signal to obtain a normalized power spectrum. To facilitate comparison with the power spectrum of Weber et al (1986), the data were also analyzed by first averaging areal biomass into 1 km bins and subdividing the resulting series into traces of 20 data points. The power estimates were then treated in the same way as above to obtain an average power spectra spanning the same scales as Weber et al (Figures 2 and 3).

A second description of spatial distribution, the semivariogram (Mackas 1984) was also computed from the same data (Figure 4). The semivariogram represents the spatial autocorrelation of krill biomass and measures the extent to which the similarity of spatial locations (or samples from those locations) is dependent on their separation.

A third, simpler descriptor, the frequency distribution of biomass estimate was finally computed for the same data set (Figure 5).

3. RESULTS

The resulting spectra shown in Figures 2 and 3 are roughly similar to the spectra of Weber et al. (1986) for krill, but much less steeper than the commonly observed spectra for chlorophyll, temperature or salinity (Steele and Henderson 1977; Lekan and Wilson 1978; Denman 1976). There is a relatively high variability of krill biomass at small scales less than 10 km that cannot be explained by the physical process only. However, the power spectra for krill biomass in the region under study is slightly steeper than that of Weber et al. (1986) in the Weddell Sea. This suggest that either a relatively more important contribution of physical processes or a relatively less important contribution of biological (behavioural) processes to the spatial distribution of krill in the Bransfield Strait-Elephant Island area in the Weddell Sea. Also our data show that at scales smaller than 1 km, the krill spectrum appears to lose its power significantly, indicating the predominance of physical processes or dispersing behaviour of krill.

The spatial autocorrelation of krill biomass (Figure 4) indicates that the variability in krill biomass between pairs of data points is only a weak function of the separation between those points. The semivariance of log biomass does not vary significantly over most distances between points except for the smallest distances. This suggests that patch size or rather a basic swarm size is smaller than 200 m, which is the finest resolution of those data.

The computed frequency of krill biomass estimate (Figure 5) is bimodal and appears to be the mixture of two lognormal distributions. About two thirds of the observations 67%) can be attributed to the first lognormal distribution (mean log (biomass)) = 0.18, SD=0.49) and one third (33%) to a second lognormal distribution (mean=1.76, SD=0.51). These two distributions may correspond to the between and within patch biomass (mean biomass between patches = 2.8 g/m^2, apparent mean biomass within patches = 115 g/m^2). Note that the biomass within swarms may be substantially higher since it appears that most swarms have a diameter smaller than 200 m and that the observed biomass is an average for a 200 m trace.

4. DISCUSSION

According to Mauchline (1980), krill form a patch, i.e. huge aggregation within a defined environmental region, of densities 1 - $10/m^3$. Environmental parameters play a more important role than behavioural reactions between individuals in maintaining the aggregation. Within a patch are found shoals, consisting of large groups of individuals. Shoals may be as large as 100 km^2 but are normally much smaller, probably in the range of 0.1-10 km. Average densities of krill in a shoal is 1-$100/m^3$. The behavioural mechanisms of the animals, rather than the physical environmental parameters, are probably more important in initiating and maintaining shoals. Cohesiveness of individuals is evident in shoals, whereas it is not generally evident in the overall structure of patches. Swarms and schools are often constituent parts of shoals. Cohesiveness reaches its greatest development in swarms and schools. They are small in spatial extent, their area being measured in square meters. Average areal sizes of 10^3-10^4 m^2 can occur, but spherical or

laminar sizes of 1-10 m^3 may be quite common. Mean densities of individuals in swarms and schools are 10^3-$10^5/m^3$. Swarms are cohesive groups of individuals without parallel orientation, while schools are cohesive groups of individuals with parallel orientation. In a swarm the centre of mass is more or less stationary relative to the ambient water, while in a school the centre of mass is mobile relative to the water.

Very little has been done on mathematical modelling the dynamics of behaviour of swarms and distribution of krill in space and time. Our data analysis suggests that most swarms (and schools) have a diameter smaller than 200 m, i.e. less than the finest resolution of those data. The result of the semivariogram (Figure 4) supports this concept. We make an attempt to model the krill biomass spectrum on the basis of the dynamical theory of krill aggregation. The basic unit of krill aggregation or shoals is assumed to be a great number of small swarms (or schools) of individual krill. They diffuse as a unit and also attract each other according to Kawasaki's (1978) model for a longrange density-dependent attraction. Krill population dynamics is also incorporated in a simple way. As a result, our basic dynamical equation for the krill concentration fluctuations is given by

$$\frac{\partial s'}{\partial t} = D\frac{\partial^2 S'}{\partial x^2} - \lambda\bar{S}\,\frac{\partial}{\partial x}\left\{\int_{-\infty}^{\infty}\phi\ (x-x')S'(x',t)dx'\right\} - \alpha\ s' + f' \qquad (1)$$

where s' (x,t): krill biomass fluctuations in space (x) and time (t), D: diffusivity for the swarm unite, $\lambda\bar{S}$: "aggregation speed" for unit swarms, α: intrinsic growth rate at stable equilibrium level $\bar{S}$, or alternatively could be interpreted as a predation rate, f': random local biomass input, and $\phi(x)$ represents a weighting function for a longrange mutual attraction of swarms.

The wavenumber spectrum of krill biomass fluctuations E(k) can be derived from (1) under the assumption that the random input function is white noise of intensity B and the weighting function $\phi(x)$ is exponential with spatial attenuation parameter c. It results

$$E^*(k) \equiv \frac{E(k)\alpha}{\pi^2 B^2} = \{Dk^2 + \alpha - \lambda\bar{S}\ c\ k^2/(k^2+c^2)\}^{-1} \qquad (2)$$

The nondimensionalized spectrum E*(k) is evaluated as a function of wavenumber k, using the following parameter values:

D = 10^3 cm^2/sec (appropriate for the basic swarm unit of the order of 10 m in size after Okubo's (1971) diffusion diagram).

α = 10^{-7}/sec (growth or predation time scale of 100 days)

c = 10^{-3}/cm (mutual attraction distance of the order of the swarm unit)

$\lambda\bar{S}$ = 1cm/sec (aggregation speed = one tenth of krill unit swimming speed).

Figure 6 shows the theoretical spectrum of krill biomass with mutual attraction (solid line), which results in a nearly uniform variance-density in the spatial scale ranging from 1 km to 20 km and relatively sharp decline in the variance below 100 m in scale, approaching the k^{-2} regime at very small scales. In the absence of the mutual attraction of swarms, on the other hand, the spectrum (broken line) decays rapidly in the spatial scale below 10 km and approaches the k^{-2} regime below 1 km. The behaviour of the theoretical spectrum agrees fairly well with that of our observation (Figure 2).

As previously discussed in this section, Mauchline's (1980) "patch within patch", or rather "swarms within schools", concept seems very adequate for interpreting the bimodality of the frequency distribution of biomass (Figure 5) and the behaviour of the semivariograms (Figure 4). To demonstrate this more precisely we have reconstructed the patch within patch model of Mangel (1987) with minor modification to account for the low "background" biomass of krill. Transect data similar to those analyzed previously were then extracted from the simulated krill spatial distribution, and the corresponding descriptors were calculated for 100 sets of 16 transects of 64 points. The results are presented in Figures 7 and 8. Not surprisingly, the resulting frequency distribution of biomass looks similar to the one obtained from the real data. The semivariogram (Figure 8) is also similar to the one from the data. The power spectrum of simulated data (Figure 9) also approximates the one obtained from the real data, although it does not mimic the apparent curvature of Figure 3 as good as the dynamical model of aggregation. Overall the simple kinematic model of Mangel appears to produce the patterns observed with real krill biomass data, and in combination with the dynamical model of krill aggregation we may be able to provide a better understanding of krill spatial distribution.

Obviously a larger set of real data need to be analyzed for testing whether or not power spectra, semivariograms, and biomass frequency distributions vary in a systematic fashion among the various subareas of the general Bransfield Strait-Elephant Island area. At the same time descriptors have to be obtained for the other relevant parameters of the integrated ecosystem model, e.g. temperature, salinity, phytoplankton biomass, and krill predators.

Another important descriptor for determination of krill population dynamics would be the frequency distribution of krill swarm size or aggregation size under given behavioural and environmental constraints. Okubo (1986) introduced the concept of the entropy of swarming, which is a measure of cohesiveness in animal aggregation. The most probably frequency distribution of animal swarm size is the one that maximized the entropy subject to given information or constraints. Thus, if the mean number of individual krill per swarm is specified, the most probably frequency distribution is geometric or exponential. Witek et al (1981) analyzed the data of krill swarms in the Antarctic Peninsula region to show that frequency of swarm size in the range of 10 to 500 m is well represented by an exponential distribution. A similar method should be employed in our data analyses.

REFERENCES

BRINTON, Edward and T. ANTEZANA. 1984. Structures of swarming and dispersed populations of krill (*Euphausia superba*) in Scotia Sea and South Shetland waters during January-March 1981, determined by bongo nets. Journal of Crustacean Biology 4 (Special 1): 45-66.

DENMAN, Kenneth L. 1976. Covariability of chlorophyll and temperature in the sea. Deep-Sea Research 23 (6): 539-550.

FASHAM, M.J.R. 1978. The application of some stochastic processes to the study of plankton patchiness. In: STEELE, J.H. (Ed.). Spatial Pattern in Plankton Communities. New York: Plenum Press. 131-156.

KAWASAKI, Kohkichi. 1978. Diffusion and the formation of spatial distribution. Mathematical Science 183: 47-52.

KOLMOGOROV, A. 1941. The local structure of turbulence in incompressible viscous fluid for very large Reynolds' numbers. Comptes rendus de l'academic des science de l"URSS 32: 16-18.

LEKAN, Jack and R.E. WILSON. 1978. Spatial variability of phytoplankton biomass in the surface water of Long Island. Estuarine and Coastal Marine Science 6: 239-250.

MACKAS, David L. 1984. Spatial autocorrelation of plankton community composition in a continental shelf ecosystem. Limnology and Oceanography 29 (3): 451-471.

MANGEL, Marc. 1987. Simulation of Southern Ocean krill fisheries. SC-CAMLR-VI/BG/22, Report for the Commission for the Conservation of Antarctic Marine Living Resources (CCAMLR), 13 October, 85 pp.

MARR, J.W. 1962. The natural history and geography of Antarctic krill Euphausia superba Dana. Discovery Report 32: 33-464.

MAUCHLINE, J. 1980. Studies on patches of krill, *Euphausia superba* Dana. BIOMASS Handbook 6, 36 pp.

OKUBO, Akira. 1971. Oceanic diffusion diagrams. Deep-Sea Research 18: 789-802.

STEELE, J.H. and E.W. HENDERSON. 1977. Plankton patches in the Northern North Sea. In: STEEL, J.H. (Ed.). Fisheries Mathematics, London-New York: Academic Press, 1-19 p.

WEBER, Larry H., S.Z. EL-SAYED and I. HAMPTON. 1986. The variance spectra of phytoplankton, krill and water temperature in the Antarctic Ocean south of Africa. Deep-Sea Research 33 (10): 1327-1343.

WITEK, Z., J. KALINOWSKI, A. GRELOWSKI nad N. WOLNOMIEJSKI. 1981. Studies of aggregations of krill (*Euphausia superba*). Meeresforsch 28: 228-243.

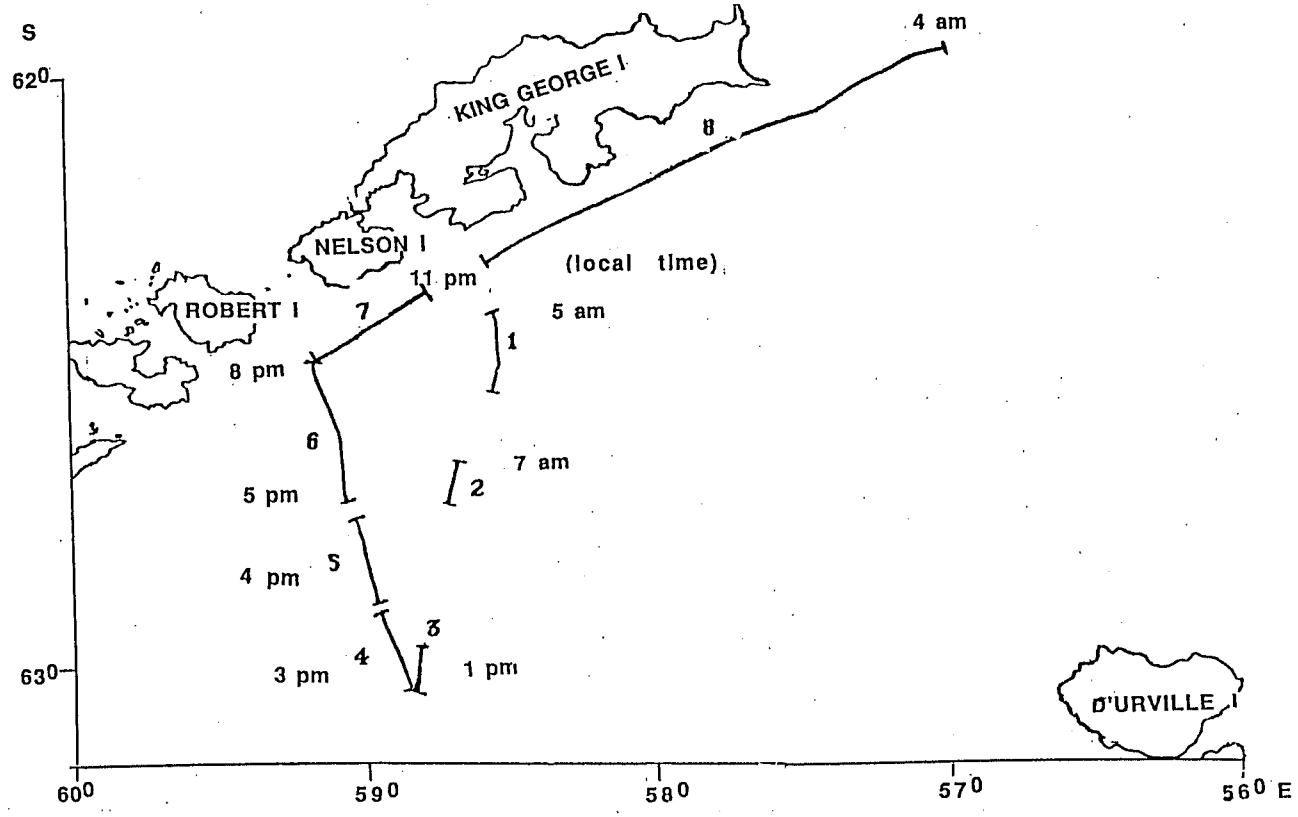

Figure 1: Location of eight transects used in the data analysis 4-5 January 1987.

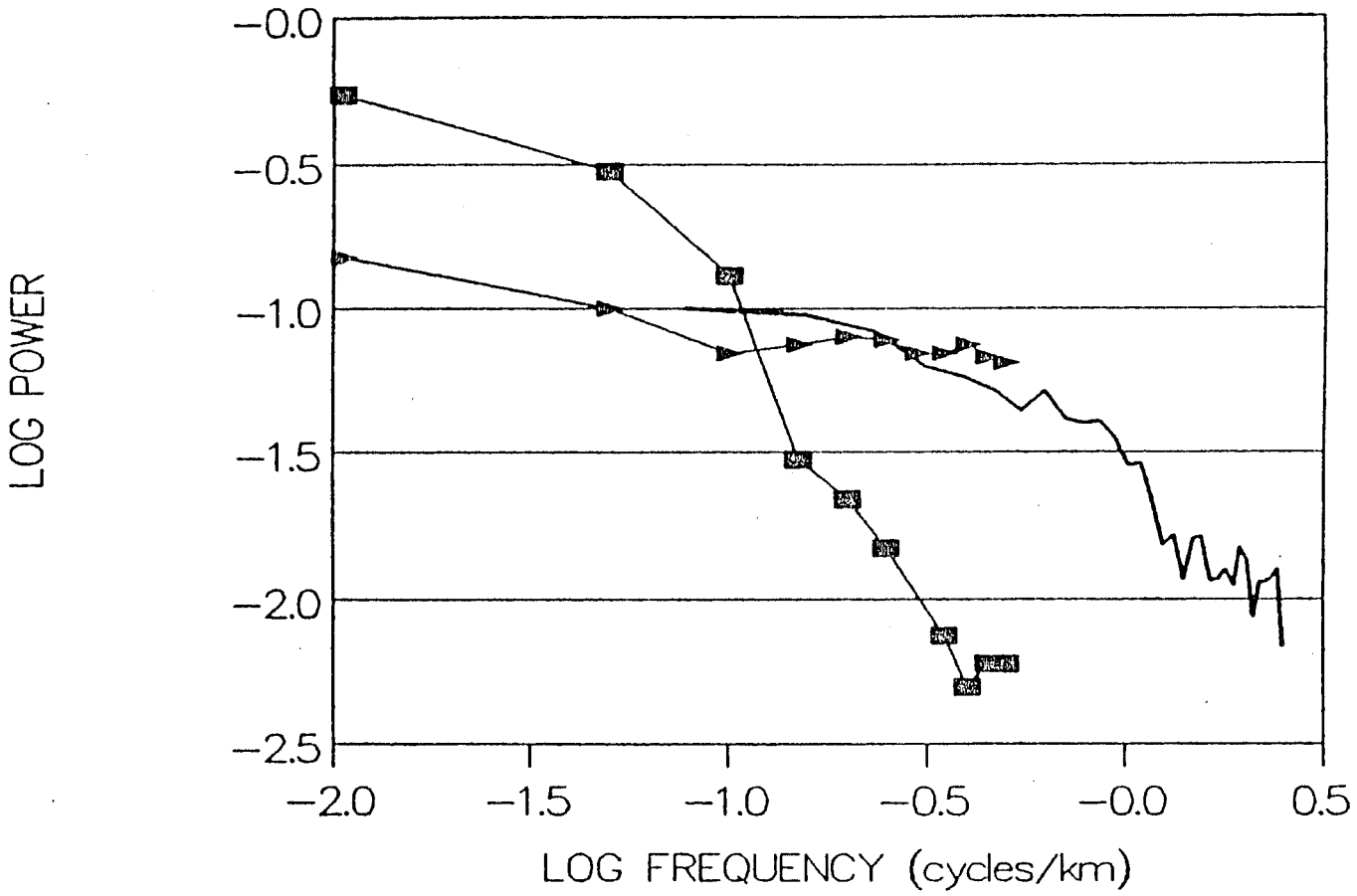

Figure 2: Normalized power spectra for chlorophyll (squares) and krill (triangles) or Weber et al (1986) and for krill acoustic data analyzed in this report (line).

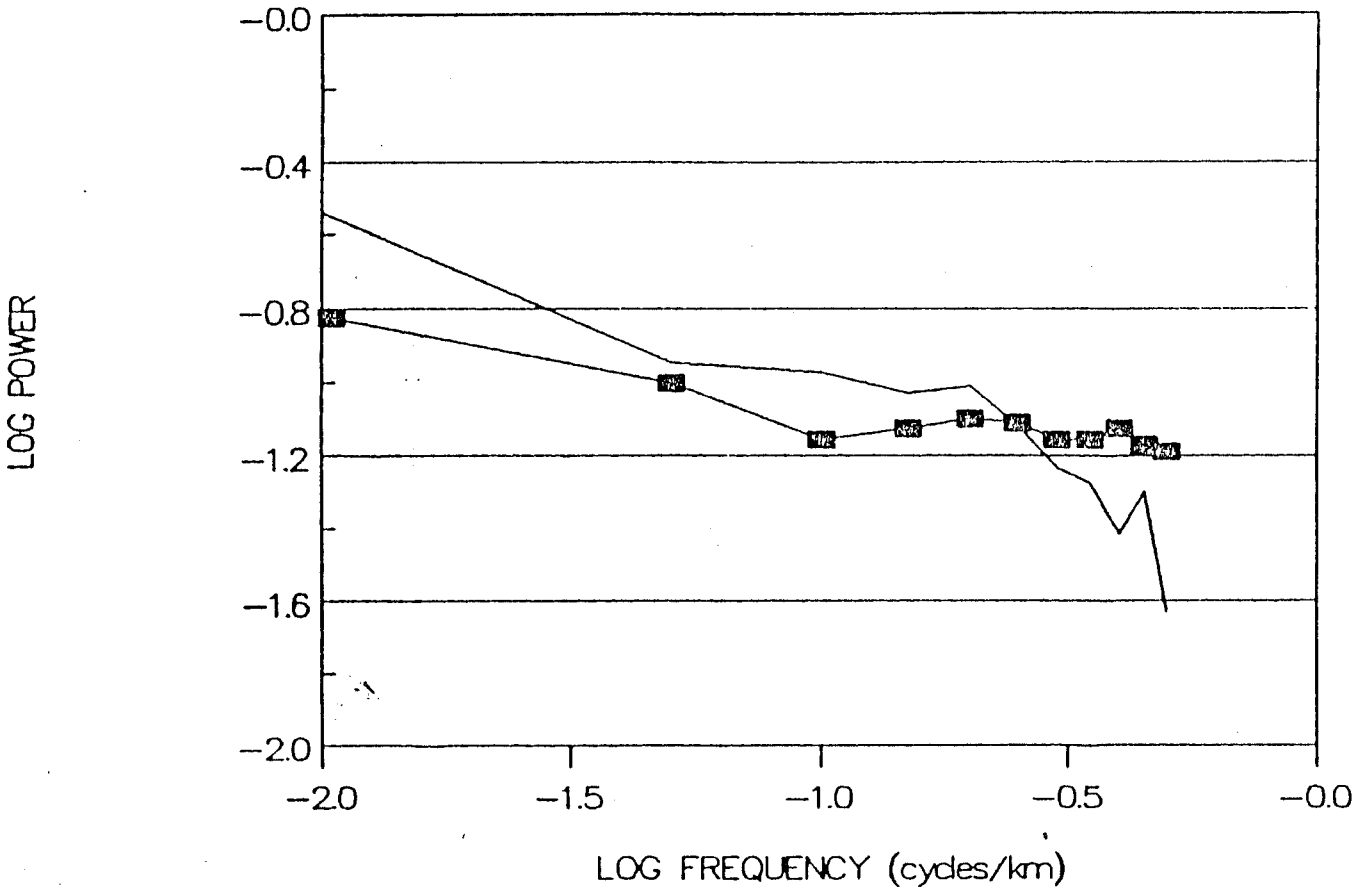

Figure 3: Power spectra for krill at the 2-20 km scale observed in this analysis (line) and by Weber et al (squares). Krill biomass was averaged over 1 km.

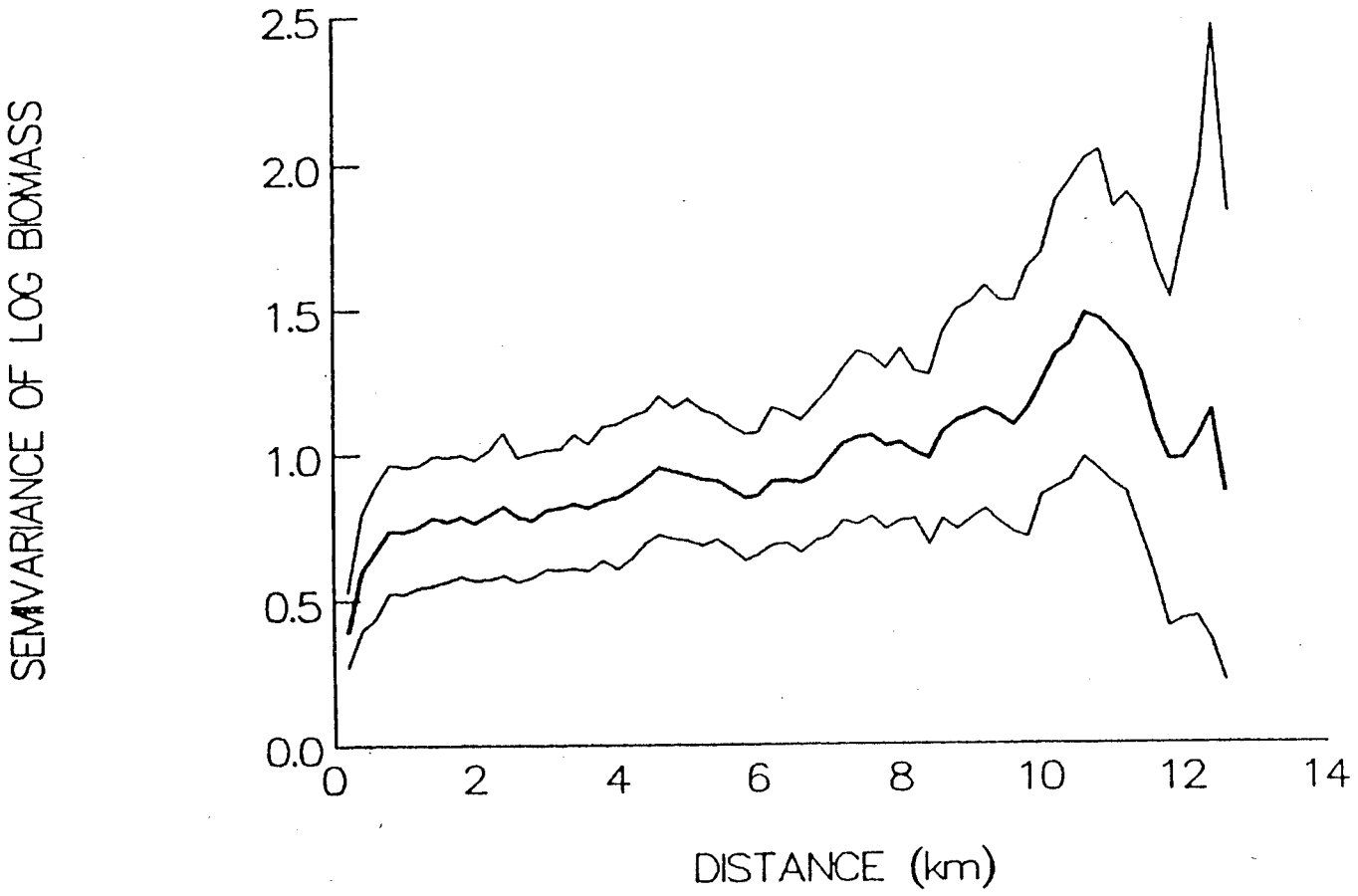

Figure 4: Semivariogram of log (krill biomass) (g/m-2) with bootstrap 95% confidence intervals for the Bransfield Strait data (4-5 January 1987).

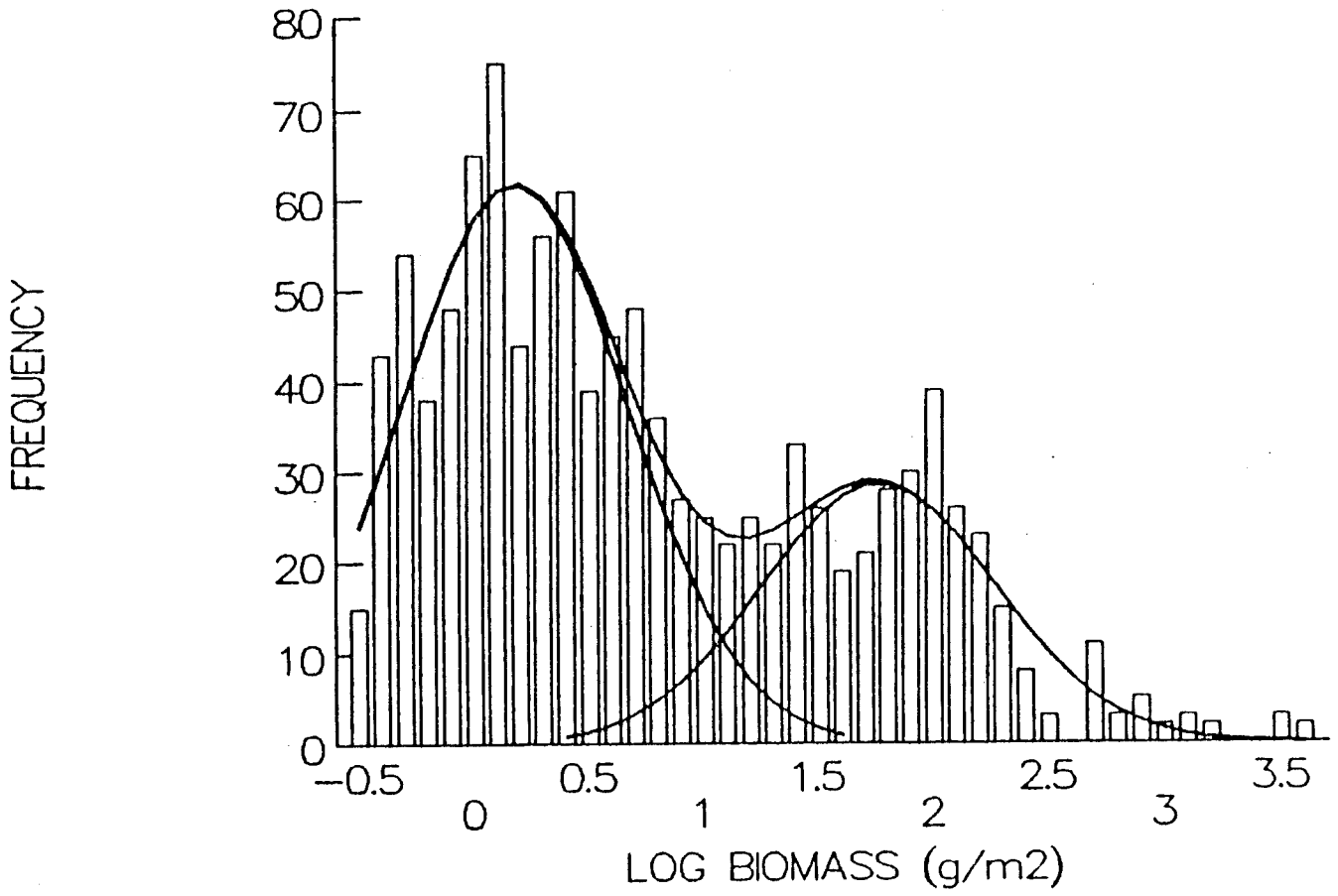

Figure 5: Frequency distribution of log (biomass estimates) (g/m^{-2}) for the Bransfield Strait data. Two lognormal distributions are fitted to the data.

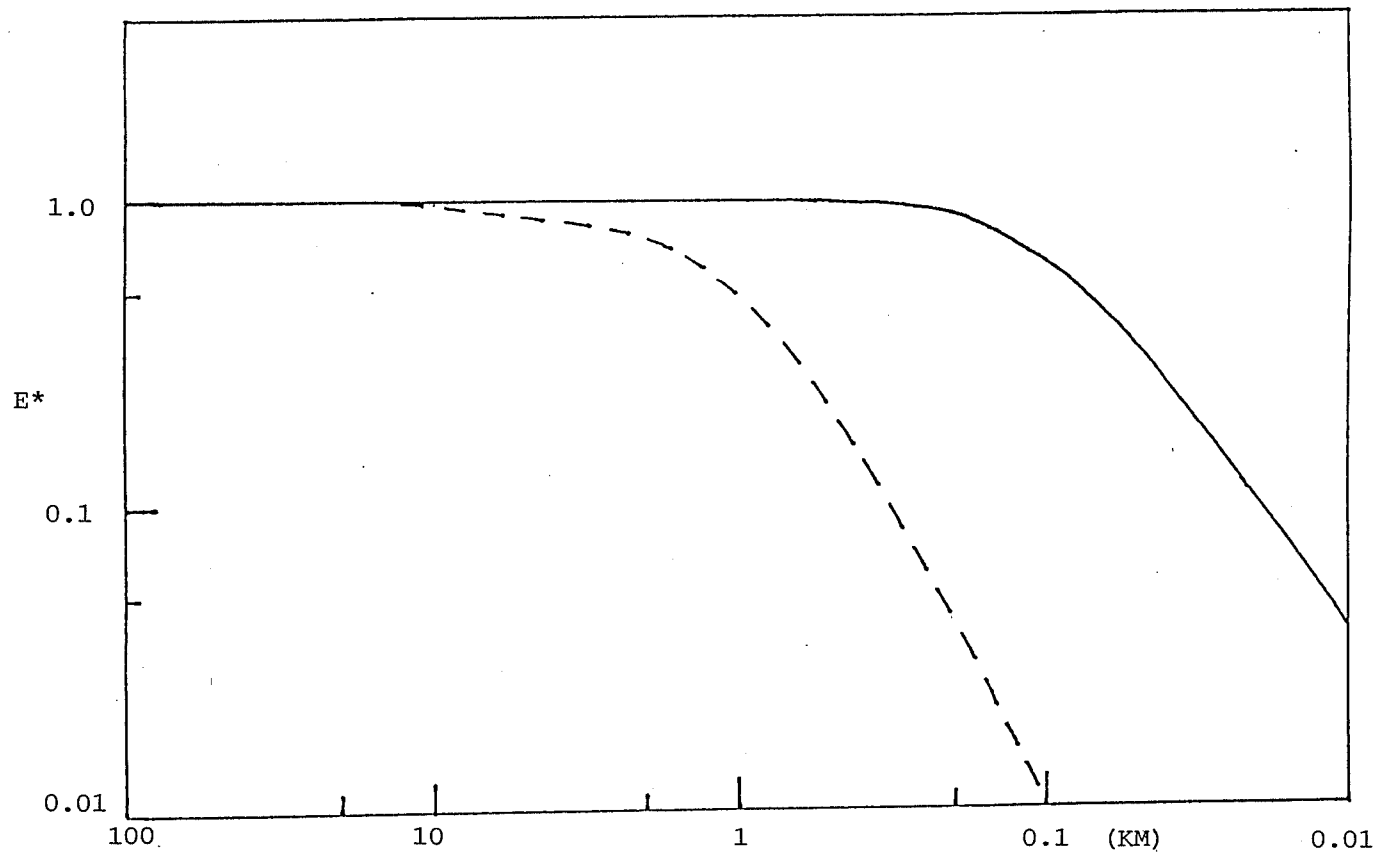

Figure 6: Normalized power spectra for krill biomass based on the dynamical theory of krill aggregation. Solid line: with mutual attraction and dispersion of basic swarm units. Broken line: without mutual attraction.

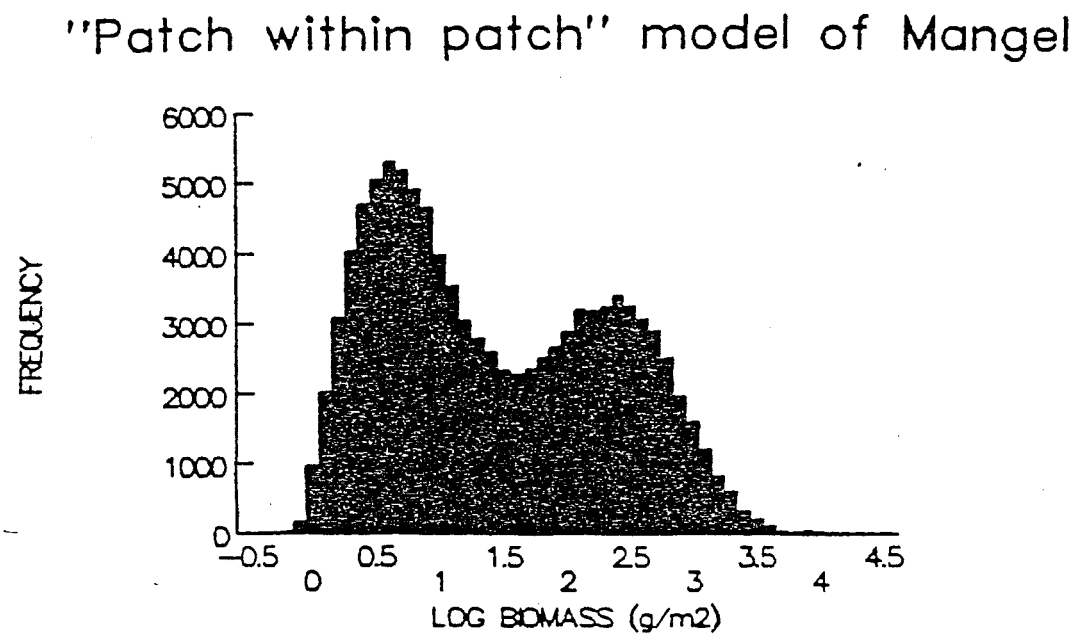

Figure 7: Frequency distribution of krill biomass based on the "patch within patch" model of Mangel (1987).

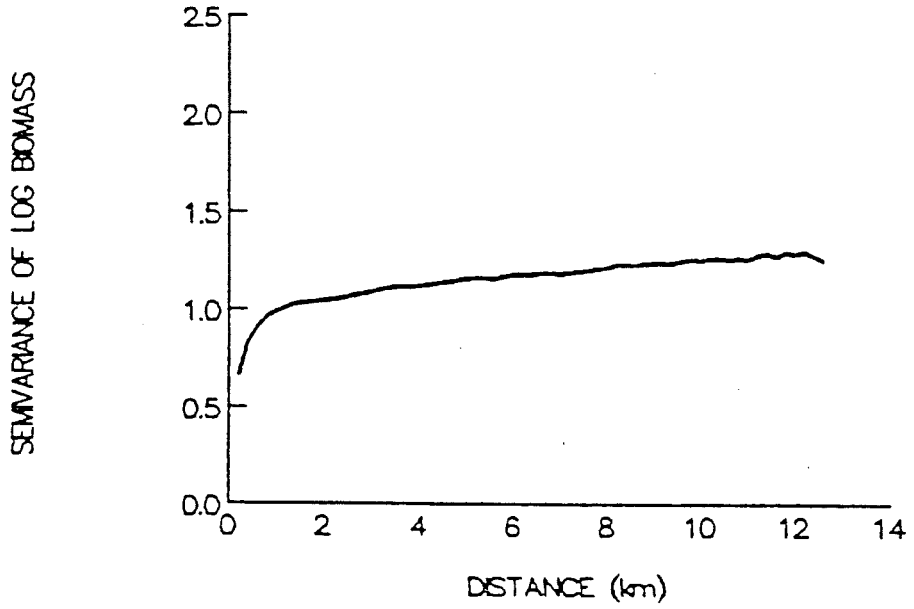

Figure 8: Semivariogram of log (krill biomass) based on the "patch within patch" model of Mangel.

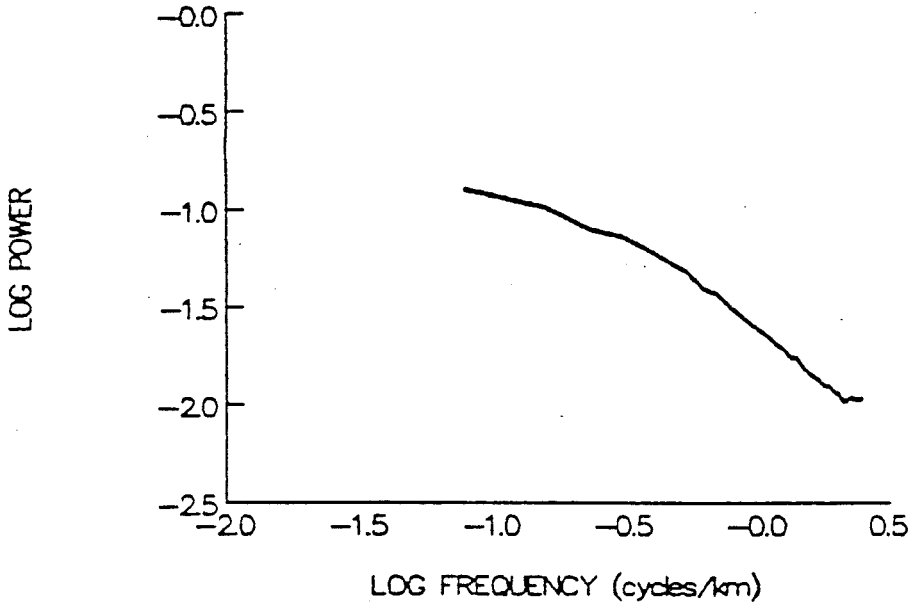

Figure 9: Power spectrum of simulated data using the "patch within patch" model of Mangel.

Légendes des figures

Figure 1 Emplacement de huit transects utilisés dans l'analyse des données les 4 et 5 janvier 1987.

Figure 2 Spectres d'intensité normalisés pour la chlorophylle (carrés) et le krill (triangles) de Weber et al. (1986) et pour les données acoustiques sur le krill analysés dans ce rapport (ligne).

Figure 3 Spectres d'intensité pour le krill sur l'échelle 2-20 km observés dans cette analyse (ligne) et par Weber et al. (carrés). La moyenne de la biomasse du krill a été prise sur 1 km.

Figure 4 Semivariogramme du logarithme (estimations de la biomasse) (g/m^2) avec une zone d'intervalles de confiance de 95% pour les données recueillies dans le détroit de Bransfield (4 au 5 janvier 1987).

Figure 5 Distribution des fréquences du logarithme (estimations de la biomasse) (g/m^2) pour les données recueillies dans le détroit de Bransfield. Deux distributions logarithmiques normales ont été ajustées aux données.

Figure 6 Spectres de puissance normalisés pour la biomasse du krill basés sur la théorie dynamique des mœurs grégaires du krill. Ligne continue: avec attraction mutuelle et dispersion des unités des essaims de base. Tireté: sans attraction mutuelle.

Figure 7 Distribution des fréquences de la biomasse du krill basée sur le modèle "regroupement à l'intérieur d'un regroupement" de Mangel (1987).

Figure 8 Semivariogramme du logarithme (biomasse du krill) basé sur le modèle "regroupement à l'intérieur d'un regroupement" de Mangel.

Figure 9 Spectre d'intensité des données de simulation utilisant le modèle "regroupement à l'intérieur d'un regroupement" de Mangel.

Подписи к рисункам

Рисунок 1 Расположение восьми гидрографических разрезов, использованных при анализе данных 4-5 января, 1987 г.

Рисунок 2 Нормализованная спектральная мощность частотного распределения (по Веберу и др., 1986 г.) для хлорофилла (квадратов) и криля (треугольников) и для проанализированных в этом отчете акустических данных по крилю (линии).

Рисунок 3 Наблюдавшиеся в этом анализе спектральные мощности частотного распределения для криля по шкале 2-20 км.(линия) и спектральные мощности, полученные путем наблюдения Вебером и др.(квадраты). Биомасса криля была усреднена по километровому квадрату.

Рисунок 4 Семивариограмма с логарифмической шкалой (биомассы криля) ($г/м^2$) с зоной доверительного интервала (95%) для данных по проливу Брансфилда (4-5 января 1987 г.).

Рисунок 5 Частотное распределение логарифма (оценок биомассы) (г/м²) для данных по проливу Брансфилда. Два логнормальных распределения приложены к данным.

Рисунок 6 Нормализованная спектральная мощность частотного распределения для криля, основанная на динамической теории агрегации криля. Постоянная линия: с взаимным притяжением и рассеянием единиц скопления. Пунктирная линия: без взаимного притяжения.

Рисунок 7 Частотное распределение биомассы криля, основанное на модели Мангела "пятна в пределах пятен" (1987 г.).

Рисунок 8 Семивариограмма логарифма (биомассы криля) основанная на модели Мангела "пятна в пределах пятен".

Рисунок 9 Спектральная мощность частотного распределения смоделированных данных при использовании модели Мангела "пятна в пределах пятен".

Leyendas de las figuras

Figura 1 Ubicación de los ocho transectos utilizados en los análisis de datos, 4-5 de enero de 1987.

Figura 2 Densidad espectral normalizada para la clorofila (cuadrados), para el krill (triángulos) de Weber et al. (1986), y para los datos acústicos del krill que se analizan en este trabajo (línea).

Figura 3 Densidad espectral del krill a la escala 2-20 km observado en este análisis (línea), y por Weber et al. (cuadrados). La biomasa del krill se promedió a lo largo de 1 km.

Figura 4 Semivariograma de log (biomasa del krill) (g/m²) con una banda de intervalos de confianza del 95% para los datos del estrecho de Bransfield (4-5 de enero de 1987).

Figura 5 Distribución de frecuencias de log (estimaciones de la biomasa) (g/m²), para los datos del estrecho de Bransfield. Las dos distribuciones logarítmicas normales se adaptan a los datos.

Figura 6 Densidades espectrales normalizadas de la biomasa del krill basados en la teoría dinámica de las concentraciones de krill. Línea solida: con atracción y dispersión mútua de las unidades básicas de cardumen. Línea quebrada: sin atracción mútua.

Figura 7 Distribución de frecuencias de la biomasa del krill basado en el modelo de Mangel (1987) de "manchas dentro de manchas".

Figura 8 Semivariograma de log (biomasa del krill) basado en el modelo de Mangel de "manchas dentro de manchas".

Figura 9 Densidad espectral de los datos simulados utilizando el modelo de Mangel de "manchas dentro de manchas".